Effect of an Organogelator on the Properties of Dental Composites

Elizabeth A. Wilder,*,† Kristen S. Wilson,† Janet B. Quinn,‡ Drago Skrtic,‡ and Joseph M. Antonucci†

Polymers Division, and Paffenbarger Research Center, American Dental Association Foundation, National Institute of Standards and Technology, Gaithersburg, Maryland 20899

Received September 22, 2004. Revised Manuscript Received March 3, 2005

Bioactive dental composites containing amorphous calcium phosphate have the potential to remineralize caries lesions and white spots, but their applications are limited by the inherent weakness of calcium phosphate as a filler material. To extend the possible uses of these materials, it is necessary to develop stable composites that exhibit strong mechanical properties and sustained ion release. Dibenzylidene sorbitol (DBS) is an organic molecule capable of inducing physical gelation in a variety of organic solvents, monomers, and polymers by forming self-assembled networks. Recent efforts have revealed that DBS is capable of gelation in a wide variety of dental monomers including an ethoxylated bisphenol A dimethacrylate (EBPADMA). This research was aimed at determining the effect of DBS networks on vinyl conversion, polymerization shrinkage, mechanical properties, and ion release potential of bioactive dental composites consisting of zirconia-modified amorphous calcium phosphate (Zr-ACP) as the primary filler phase and EBPADMA as the resin matrix phase. Although DBS had little effect on the vinyl conversion of EBPADMA/Zr-ACP composites, it significantly (1) reduced the volumetric shrinkage and associated shrinkage stress, and (2) increased the biaxial flexural strength and hardness of dry specimens. However, ion release studies suggest that DBS inhibits the release of calcium and phosphate ions.

Introduction

Bioactive polymeric dental materials containing amorphous calcium phosphate (ACP) have tremendous appeal due to both (i) their potential for remineralizing defective mineralized tissues such as enamel, dentin, and bone,[1−5] and (ii) their biocompatibility.[6] In aqueous environments, ACP converts readily to hydroxyapatite,[6] the major mineral component of teeth and bones. In addition to potential use as pit and fissure sealants and base liners underneath other restorations, the possible applications of ACP composites also extend to endodontic and periodontal applications where these materials could be used to promote healthy bone growth. However, current applications of these materials are limited by the inherent weakness of ACP as a filler for polymeric composites.[7]

Although the mechanical properties of synthetic calcium phosphates may be improved by incorporating them into polymers, the polymer matrixes introduce their own set of complications. Polymeric composites are subject to the shortcomings of the resin matrix phase including shrinkage during polymerization and incomplete vinyl group conversion.[8] These are two significant problems not encountered with nonpolymeric dental materials such as amalgams or self-setting calcium phosphate cements.[9] Polymerization shrinkage can lead to poor internal and external adhesion as well as morphological defects including structural cracks and flaws due to stress development in the composite. Incomplete vinyl conversion raises biocompatibility concerns due to potential leaching of monomers and other unbound species into the oral environment.

Traditional glass-based composite materials are used in a wide range of dental applications including restoration of incisal edges and occlusal surfaces of anterior teeth, full crowns, cusp buildups, and in some posterior restorations.[10] The composites are therefore subject to a wide variety of chemical, biochemical, mechanical, and thermal challenges attributable to a hostile oral environment and repetitive masticatory stresses.[11] Whereas glass- or ceramic-filled composites may exhibit flexural moduli up to 15 000 MPa and flexural strengths on the order of 150 MPa, ACP-filled composites typically exhibit much lower flexural moduli of approximately 3000 MPa and flexural strengths on the order of 50 MPa. Although ACP-based composites may never be

* Corresponding author. Tel: 301-975-6786. Fax: 301-975-4977. E-mail: elizabeth.wilder@nist.gov.
† Polymers Division.
‡ Paffenbarger Research Center.

(1) Antonucci, J. M.; Skrtic, D.; Eanes, E. D. *Abstr. Pap.−Am. Chem. Soc.* **1994**, *207*, 60-BTEC.
(2) Antonucci, J. M.; Skrtic, D.; Eanes, E. D. *Abstr. Pap.−Am. Chem. Soc.* **1995**, *209*, 6-MACR.
(3) Antonucci, J. M.; Skrtic, D.; Eanes, E. D. In *Hydrogels and Biodegradable Polymers for Bioapplications*, 1996; Vol. 627, pp 243−254.
(4) Antonucci, J. M.; Skrtic, D.; Eanes, E. D. *Abstr. Pap.−Am. Chem. Soc.* **1998**, *216*, U121−U121.
(5) Antonucci, J. M.; Skrtic, D. *Abstr. Pap.−Am. Chem. Soc.* **2001**, *222*, U421−U421.
(6) Skrtic, D.; Antonucci, J. M.; Eanes, E. D. *J. Res. Natl. Inst. Stand. Technol.* **2003**, *108*, 167−182.
(7) Skrtic, D.; Antonucci, J. M.; Eanes, E. D.; Eidelman, N. *Biomaterials* **2004**, *25*, 1141−1150.
(8) Skrtic, D.; Stansbury, J. W.; Antonucci, J. M. *Biomaterials* **2003**, *24*, 2443−2449.
(9) Chow, L. C. In *Octacalcium Phosphate. Monographs of Oral Science*; Chow, L. C., Eanes, E. D., Eds.; Karger: Basel, Switzerland, 2001.
(10) Kim, O.; Shim, W. J. *Polym. Compos.* **2001**, *22*, 650−659.
(11) Lim, B.-S.; Ferracane, J. L.; Condon, J. R.; Adey, J. D. *Dent. Mater.* **2002**, *18*, 1−11.

10.1021/cm048340x
Published on Web 04/29/2005

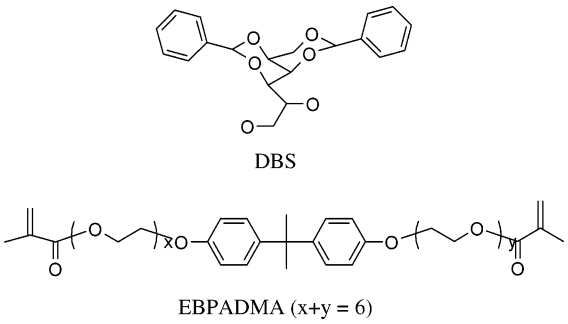

Figure 1. Structures of 1,3:2,4-dibenzylidene-D-sorbitol and ethoxylated bisphenol-A dimethacrylate.

able to compete with their glass-filled counterparts, more modest improvements in their stability and mechanical properties could extend the now-limited applications of these bioactive materials.

Methods to improve the strength and stability of ACP composites have included modification of ACP with silica or zirconia precursors,[7] the use of silane coupling agents,[3] and variations in the resin composition.[7,12] There have also been efforts to increase the stability of ACP as a filler phase with additives that introduce magnesium, carbonate, or pyrophosphate[13] into the structure of ACP or to utilize other types of calcium phosphates such as vitreous calcium metaphosphates as alternatives to ACP.[14] While there have been some promising developments with bioactive composites based on ACP, current formulations remain limited in their applications because of their deficiencies with regard to mechanical properties, polymerization shrinkage, and stress development.

Low-molecular-weight organic gelators (LMOGs), a class of organogelators, have garnered significant attention due to their ability to self-assemble and promote gelation in a variety of organic solvents and polymer melts.[15−17] Dibenzylidene sorbitol (DBS), shown in Figure 1, is a LMOG capable of inducing physical gelation in a wide variety of organic solvents and polymer melts by forming rigid three-dimensional networks.[18−30] DBS is a relatively benign material that is already in use in cosmetic applications.[31,32] Recent efforts in this laboratory have found that DBS is capable of gelling a wide variety of dental monomers including monofunctional monomers such as methyl methacrylate, benzyl methacrylate, and 2-hydroxyethyl methacrylate, as well as difunctional monomers including ethoxylated bisphenol A dimethacrylate (EBPADMA), poly(ethylene oxide) dimethacrylate, 1,6-hexamethylene dimethacrylate, tetra(ethylene glycol) dimethacrylate, and tri(ethylene glycol) dimethacrylate. This research was aimed at determining the effect of DBS networks on vinyl conversion, polymerization shrinkage, and the mechanical strength of dental polymers and bioactive dental composites containing zirconia-modified ACP (Zr-ACP) in a matrix derived from the photocuring of an EBPADMA (Figure 1).

Materials and Methods

Synthesis of Zr-ACP. Zr-ACP filler was prepared as follows: 9.51 g of sodium phosphate (GFS Chemicals, Powell, OH) and 0.61 g of sodium pyrophosphate (J. T. Baker, Phillipsburg, NJ) were dissolved with vigorous mechanical mixing in 58 mL of distilled water and 67 mL of 1 mol/L sodium hydroxide for approximately 15 min. To this solution, 21.3 g of calcium nitrate tetrahydrate (Sigma-Aldrich Corp, St. Louis, MO), dissolved in 85 mL of distilled water and 40 mL of a 0.25 mol/L zirconyl chloride (GFS) solution were simultaneously added resulting in instant precipitation. After approximately 5 min of mixing, the precipitated Zr-ACP was washed with ammoniated water and cold acetone, vacuum-filtered, and then lyophilized for 24 h according to a previously described method.[33] The average particle size of Zr-ACP prepared by this method has been reported as (5.9 ± 0.7) μm,[34] although the particles tend to aggregate during synthesis and subsequent mixing with the resin phase. The amorphous state of the lyophilized Zr-ACP was verified by X-ray diffraction (XRD) and Fourier transform infrared spectroscopy (FTIR). FTIR tests were performed by mixing approximately 0.5 mg of the Zr-ACP with 4 mg of potassium bromide powder (Spectra-Tech, Inc., Shelton, CO) and pressing them into circular pellets which were analyzed with a Nicolet Magna-IR FTIR System spectrophotometer (Nicolet Instrument Corporation, Madison, WI). XRD profiles were taken on a Rigaku X-ray diffractometer (Rigaku/USA Inc., Danvers, MA) operated at 40 kV and 40 mA.

Sample Preparation. To prepare the organogel-modified samples, various amounts of DBS (Milliken Chemicals, Spartanburg, SC) were dissolved into approximately 10 g of the liquid monomer ethoxylated bisphenol A dimethacrylate (EBPADMA, degree of ethoxylation = 6) (Esstech, Essington, PA) by adding the DBS to the monomer and storing it in an oven at 100 °C for 2 h. Upon cooling, the DBS self-assembled causing gelation of the liquid monomer.

(12) Antonucci, J. M.; McDonough, W. G.; Liu, D. W.; Skrtic, D. *Abstr. Pap.—Am. Chem. Soc.* **2003**, *225*, U664−U664.
(13) Skrtic, D.; Eanes, E. D.; Antonucci, J. M. In *Industrial Biotechnological Polymers*; Gebelein, C. G., Carraher, C. E. J., Eds.; Technomic Publishing Company: Lancaster, PA, 1995.
(14) Antonucci, J. M.; Fowler, B. O.; Venz, S. *Dent. Mater.* **1991**, *7*, 124−129.
(15) Terech, P.; Weiss, R. G. *Chem. Rev.* **1997**, *97*, 3133−3159.
(16) Gronwald, O.; Snip, E.; Shinkai, S. *Curr. Opin. Colloid Interface Sci.* **2002**, *7*, 148−156.
(17) Abdallah, D. J.; Weiss, R. G. *J. Braz. Chem. Soc.* **2000**, *11*, 209−218.
(18) Yamasaki, S.; Tsutsumi, H. *Bull. Chem. Soc. Jpn.* **1994**, *67*, 906−911.
(19) Yamasaki, S.; Tsutsumi, H. *Bull. Chem. Soc. Jpn.* **1994**, *67*, 2053−2056.
(20) Yamasaki, S.; Tsutsumi, H. *Bull. Chem. Soc. Jpn.* **1995**, *68*, 123−127.
(21) Yamasaki, S.; Ohashi, Y.; Tsutsumi, H.; Tsujii, K. *Bull. Chem. Soc. Jpn.* **1995**, *68*, 146−151.
(22) Mercurio, D. J.; Khan, S. A.; Spontak, R. J. *Rheol. Acta* **2001**, *40*, 30−38.
(23) Mercurio, D. J.; Spontak, R. J. *J. Phys. Chem. B* **2001**, *105*, 2091−2098.
(24) Fahrländer, M.; Fuchs, K.; Friedrich, C. *J. Rheol.* **2000**, *44*, 1103−1119.
(25) Fahrländer, M.; Fuchs, K.; Mülhaupt, R.; Friedrich, C. *Macromolecules* **2003**, *36*, 3749−3757.
(26) Ilzhoefer, J. R.; Broom, B. C.; Nepa, S. M.; Vogler, E. A.; Khan, S. A.; Spontak, R. J. *J. Phys. Chem.* **1995**, *99*, 12069−12071.
(27) Ilzhoefer, J. R.; Spontak, R. J. *Langmuir* **1995**, *11*, 3288−3291.
(28) Wilder, E. A.; Hall, C. K.; Spontak, R. J. *J. Colloid Interface Sci.* **2003**, *267*, 509−518.
(29) Wilder, E. A.; Braunfeld, M. B.; Jinnai, H.; Hall, C. K.; Agard, D. A.; Spontak, R. J. *J. Phys. Chem. B* **2003**, *107*, 11633−11642.
(30) Wilder, E. A.; Hall, C. K.; Khan, S. A.; Spontak, R. J. *Langmuir* **2003**, *19*, 6004−6013.
(31) Kasat, R. B.; Lee. W.; McCarthy, D. R.; Telhan, N. G. U.S. Patent 5,490,979, 1996.
(32) Schamper, T.; Jablon, M.; Randhawa, M. H.; Senatore, A.; Warren, J. D. *J. Soc. Cosmetic Chem.* **1986**, *37*, 225−231.
(33) Skrtic, D.; Antonucci, J. M.; Eanes, E. D.; Brunworth, R. T. *J. Biomed. Mater. Res.* **2002**, *59*, 597−604.
(34) Lee, S.-Y.; Regnault, W. F.; Antonucci, J. M.; Skrtic, D. **2005**, in press.

Table 1. Sample Compositions

sample	% filler in sample (DBS + Zr-ACP)	% DBS in sample	% DBS in EBPADMA	% EBPADMA in sample	% Zr-ACP in sample
1a	0	0	0	100	0
1b	5	5	5	95	0
1c	10	10	10	90	0
2a	40	0	0	60	40
2b	40	3.1	5	60	36.9
2c	40	6.60	10	60	33.4
3a	40.00	0	0	60.00	40
3b	42.97	2.97	5	57.00	40
3c	44.76	4.76	8	55.24	40
3d	45.94	5.94	10	54.06	40
4	45.82	2.82	5	54.18	43
5	47.72	2.72	5	52.28	45

To activate the EBPADMA for visible light photopolymerization, 0.2% by mass fraction of camphorquinone (Sigma-Aldrich) and 0.8% by mass fraction of ethyl 4-*N*,*N*-dimethylaminobenzoate (Sigma-Aldrich) were added to the EBPADMA or the EBPADMA/DBS solutions (prior to gelation for ease of mixing) and heated at 60 °C for approximately 30 min to completely dissolve the photoinitiators. Composite specimens containing Zr-ACP were prepared by mixing the activated EBPADMA or EBPADMA/DBS gels with 30% to 45% by mass fraction Zr-ACP.

Three main sets of samples as well as two additional formulations were prepared and are summarized in Table 1. The first set of samples consisted of EBPADMA with 0, 5, or 10% by mass fraction DBS without any Zr-ACP, the second set contained a constant filler (DBS + Zr-ACP) loading of 40%, and the third set contained a constant Zr-ACP loading of 40%. Samples 4 and 5 had 43% and 45% Zr-ACP, respectively, and 5% DBS, and were used in the shrinkage and stress measurements to determine the effect of additional filler. It should be noted that samples 2a and 3a were identical, but are separated in the table for clarity. Unless otherwise noted (e.g., the shrinkage and stress measurements), the DBS concentrations were calculated with respect to the EBPADMA, while the Zr-ACP and filler concentrations were calculated with respect to the total sample weight.

Rheology. Rheological measurements were performed on an Advanced Rheometric Expansion System (ARES, Rheometric Scientific, Piscataway, NJ). Tests on the EBPADMA (as-received) were performed using 50-mm cone and plate geometry with a cone angle of 0.04 rad. Steady rate sweeps were performed with a 300-s measurement time from 1/s to 50/s. Measurements on gelled EBPADMA specimens containing 5% DBS were run using 25-mm parallel plate geometry. Frequency sweeps were conducted at 0.1% strain from 0.01 rad/s to 200 rad/s to calculate the elastic or storage modulus (G') and the viscous or loss modulus (G'').

Conversion Measurements. Vinyl group conversion was measured using mid-FTIR[35] by monitoring the reduction in the C═C vinyl band (1637 cm^{-1}) in comparison to an unchanged aromatic band (1583 cm^{-1}) used as an internal standard. A drop of the sample was spread between two KBr plates and after an initial spectrum was taken, the specimen was cured (i.e., polymerized) within the KBr plates with visible light (λ = 470 nm) 60 s per side (Triad 2000, Dentsply, York, PA). At least 3 specimens per sample were used to determine an average vinyl conversion. Measurements were taken before cure, immediately after cure, and 24 h post-cure.

Mechanical Testing. Biaxial flexural strength (BFS) measurements were performed at a crosshead speed of 0.5 mm/min using a computer-controlled universal testing machine (Instron 5500R, Instron Corp, Canton, MA) with TestWorks4 software. The BFS tests were performed on disk specimens (5 or more per sample) approximately 15 mm in diameter × 1 mm thick. Specimen disks were prepared by spreading the sample into circular molds that were subsequently sandwiched between two Mylar films and clamped between two glass slides. The specimens were cured 60 s per side with visible light (Triad 2000, Dentsply, York, PA) and then stored for 24 h at 37 °C before testing. Surfaces of the fractured specimens were examined using a stereomicroscope (Leica WILD M10, Leica Microsystems AG, Heerbrugg, Switzerland).

Knoop Hardness Values. Knoop hardness values were obtained by indenting broken, tested BFS specimens. For each DBS content (0, 5, 8, and 10% by mass fraction), the pieces of four different broken specimens were randomly selected for indentation. Three indents were randomly placed on each of the selected pieces, for a total of 48 indentations altogether, or twelve per DBS content. The tests were made on a Tukon 300FMDF Wilson/Instron hardness machine (Canton, MA), with load, P, of 200 g. The indentation diagonals, d, were measured with an optical system attached to the microscope, and Knoop hardness was calculated by $KH = 14.229\ P/d^2$.

Volumetric Shrinkage. To measure volumetric shrinkage, approximately 0.9−1.0 mg of the composite specimen (3 or more specimens per sample) was placed on a 1-mm-thick glass slide and positioned so that the specimen was centered inside the socket rim of a glass joint of a computer-controlled mercury dilatometer.[36] A clamp was used to ensure a tight seal between the slide and the rim, and the socket was subsequently filled with mercury. A plunger connected to a linear variable displacement transducer (LVDT) was lowered to float on the mercury meniscus. A thermistor attached to the socket of the glass joint was employed to measure temperature changes while the LVDT monitored any changes in the height of the mercury. After the LVDT reached steady state, the specimen was cured for 60 s (Max Lite; Caulk/Dentsply, Milford, DE) and the thermistor and LVDT measurements were taken for 60 min. The curing light was then triggered for an additional 30 s. Volumetric shrinkage corrected for temperature fluctuation was plotted as a function of time, and the overall shrinkage due to curing was determined based on the mass and density of the polymer specimen. Sample densities were measured by the Archimedes principle with a microbalance equipped with a water immersion bath that allowed for specimens to be weighed both dry and submerged (Sartorious YDK01 Density Determination Kit; Sartorious AG, Goettingen, Germany).

Maximum Stress. Maximum curing stress was measured using a cantilever-beam tensometer. A cylindrical specimen (minimum three specimens per sample) approximately 2.5 mm high and 6 mm in diameter was inserted between two cylindrical glass rods that had been silanized with a solution of 1% mass fraction of 3-methacryloxypropyltrimethoxysilane in acetone. The upper rod was connected to a cantilever with an LVDT to measure height displacements resulting from curing while the lower rod was stationary. A curing light (Caulk/Dentsply, Milford, DE) placed under the lower rod was triggered for 60 s to cure the specimen, and the displacement of the upper rod was followed from the onset of curing to 60 min afterward to monitor stress development. Calibration of the tensometer revealed a compliance of (7.176 ± 0.008) N/μm that was taken into account during the calculations.

Ion Release. Disk specimens (four specimens per sample) were prepared in the same manner as for the BFS testing described previously. Each disk was suspended by a wire frame in 95 mL of a continuously stirred saline solution buffered (pH = 7.4) with *N*-2-hydroxyethylpiperazine-*N*′-2-ethanesulfonic acid (HEPES). Over a period of 30 d, 2-mL aliquots were taken at various intervals.

(35) Stansbury, J. W.; Dickens, S. H. *Dent. Mater.* **2001**, *17*, 71−79.

(36) Skrtic, D.; Antonucci, J. M.; Eichmiller, F. C.; Stansbury, J. W. *J. Dent. Res.* **2000**, *79*, 366−366.

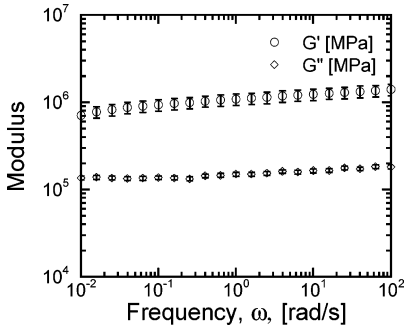

Figure 2. Frequency sweep of EBPADMA with 5% by mass fraction DBS.

Table 2. Vinyl Group Conversion Percentage of EBPADMA and EBPADMA/Zr-ACP Composites Immediately Post-Irradiation and 24-h Post-Irradiation (Standard Deviations Shown in Parentheses)

sample	post-irradiation conversion	24-h conversion
1a	88.9 (0.9)$^{A\,a}$	90.8 (0.7)^{A,C}
1b	93.0 (1.6)^{B,C}	95.4 (0.8)^{B}
1c	92.4 (1.2)^{B,C}	94.4 (0.8)^{B}
2a	74.6 (0.7)^{D,I}	77.6 (0.3)^{G}
2b	78.2 (0.9)^{E,G}	80.2 (1.0)^{E,H}
2c	81.7 (1.3)^{F,H}	83.3 (1.8)^{F}
3a	74.6 (0.7)^{D,I}	77.6 (0.3)^{G}
3b	73.2 (1.0)^{D}	76.2 (0.5)^{G,I}
3d	73.2 (1.7)^{D}	76.4 (2.2)^{G,I}

[a] Different superscript capital letters indicate statistical differences ($P < 0.05$).

Calcium ion and phosphate ion concentrations were measured using spectrophotometric methods described in detail elsewhere[7,37,38] using a Cary model 219 spectrophotometer (Varian Analytical Instruments, Palo Alto, CA). After soaking, the composite specimens were dried with a laboratory towel to remove surface water, weighed, tested for their biaxial flexural strength, and analyzed by XRD.

Statistical Analyses. Data were analyzed using one-way ANOVA and the Tukey "Honestly Significant Difference" (HSD) test. Differences were considered significant when $P < 0.05$. In the data presentations that follow, error bars and ± symbols indicate one standard deviation in each direction, where the standard deviation is taken as a measure of the standard uncertainty.

Results and Discussion

The as-received EBPADMA flowed easily at room temperature and had a viscosity of (0.529 ± 0.001) Pa·s as determined through a steady rate sweep. Addition of 5% DBS resulted in physical gelation[39] with $G' > G''$ and both G' and G'' considered to have little dependence on frequency as shown in Figure 2.

FTIR results, shown in Table 2, indicate that adding DBS to EBPADMA resulted in a modest and statistically significant increase in vinyl group conversion of samples without Zr-ACP. This may have been due to the "gel" or "Trommsdorff" effect[40,41] that suggests that polymerization kinetics can increase at high viscosities due to a reduction in chain termination accompanying the decreased mobility of the polymer radicals. DBS, by causing physical gelation of the monomer in a manner analogous to chemical gelation, may also reduce the mobility of the chain ends, thereby enhancing free radical propagation and vinyl conversion. Future efforts may include real-time infrared spectroscopy to monitor the kinetics of polymerization. Differences in vinyl conversion between samples with 5 and 10% DBS were insignificant, suggesting that higher loadings do not lead to further improvements in conversion. This may be due to the presence of air voids within the high-viscosity EBPADMA/DBS gels as well as reduced clarity at higher DBS loadings, both of which may partially inhibit photocuring. Additionally, systems containing 10% DBS may have had such high viscosities that the positive effects of gelation were nullified by inhibition of the propagation step during polymerization.

Results for composite samples with constant filler loadings of 40% by mass fraction show a small but statistically significant increase in conversion upon addition of DBS, but this may likely be attributed to the relative decrease in the amount of Zr-ACP. The systems containing Zr-ACP had consistently lower conversions than samples without Zr-ACP, indicating that Zr-ACP interferes with the curing of EBPADMA. In samples with a constant Zr-ACP loading of 40%, there were no significant differences between samples with and without DBS. Accordingly, while DBS may improve the conversion of EBPADMA, DBS does not appear to have a significant effect on the conversion of EBPADMA/Zr-ACP composites. This could be due to disruption of the DBS gel structure during mixing with the Zr-ACP filler, or it may be that the viscosity of the EBPADMA/Zr-ACP composites is high enough to mask any effect of the DBS network.

Table 3. Biaxial Flexural Strength of Dry, Cured EBPADMA and EBPADMA/Zr-ACP Composites (Standard Deviations Shown in Parentheses)

sample	BFS [MPa]
1a	160 (16)$^{A\,a}$
1b	149 (27)^{A}
3a	59.5 (5.7)^{B}
3b	83.0 (3.7)^{C}
3c	74.6 (5.1)^{D}
3d	69.6 (4.4)^{D}

[a] Different superscript capital letters indicate statistical differences ($P < 0.05$).

Results from the mechanical testing on dry specimens (Table 3) reveal that the addition of DBS did not significantly affect the BFS of the cured EBPADMA. However, addition of Zr-ACP significantly reduced the BFS of the cured EBPADMA. This is expected due to the inherently brittle nature of the Zr-ACP and the lack of chemical or strong physical interactions between Zr-ACP and EBPADMA. Addition of 5% by mass fraction DBS to the EBPADMA/Zr-ACP composites resulted in an almost 40% increase to the BFS, raising it from (59.5 ± 5.7) to (83 ± 3.0) MPa. Adding 10% by mass fraction of DBS significantly decreased the BFS compared to the sample containing 5% DBS. Fractographic analyses indicate that the reduction in BFS at higher loadings is due to the nature of voids incorporated

(37) Murphy, J.; Riley, J. P. *Anal. Chim. Acta* **1962**, *27*, 31−36.
(38) Vogel, G. L.; Chow, L. C.; Brown, W. E. *Caries Res.* **1983**, *17*, 23−31.
(39) Kavanagh, G. M.; Ross-Murphy, S. B. *Prog. Polym. Sci.* **1998**, *23*, 533−562.
(40) Schildknecht, C. E. In *Polymer Processes*; Schildknecht, C. E., Ed.; Interscience Publishers: London, 1956; Vol. X, pp 31−68.
(41) Matyjaszewski, K. In *Handbook of Radical Polymerization*; Matyjaszewski, K., Davis, T. P., Eds.; John Wiley and Sons: Hoboken, NJ, 2002; pp 361−406.

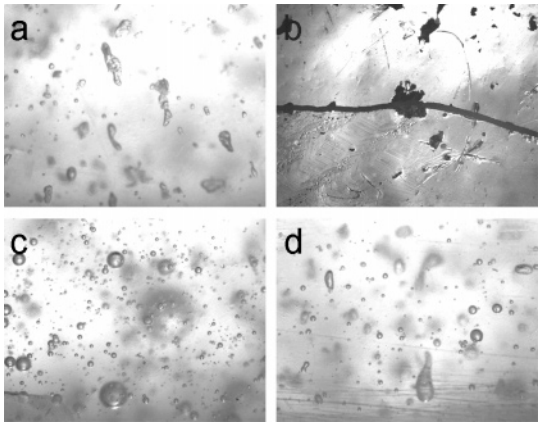

Figure 3. Fractographic analyses of EBPADMA/Zr-ACP composites containing (a and b) 0% by mass fraction DBS, (c) 5% by mass fraction DBS, and (d) 10% by mass fraction DBS.

into the resin during mixing of the viscous EBPADMA/DBS gel with Zr-ACP.

Nonductile fracture initiates at the site of flaws, and the strength is dependent on the size and shape of the flaw as well as the local stress. The samples containing 0% by mass fraction DBS were found to contain jagged, irregularly shaped pores, with many located at the specimen tensile surfaces. These pores or voids were formed by air introduced during the mixing process. Often air or gases trapped within a material will form round, smooth pores to minimize surface energy, and then rise to the surface. If the material is too viscous, the voids may be irregular and remain trapped within the material. Figure 3a shows the pore distribution within these translucent specimens. During the biaxial flexural testing, five of the six specimens that contained 0% by mass fraction DBS failed at these rough pores. The sixth (and strongest) specimen had no rough pores in the vicinity of the highest stress and failed instead at a smooth, spherical pore just beneath the surface. Figure 3b shows a typical rough pore at the failure site of a specimen containing 0% by mass fraction DBS.

The specimens containing 5% by mass fraction DBS contained many large pores, but they were smooth and spherical, as shown in Figure 3c. Figure 3d shows the pore distribution of the samples containing 10% by mass fraction DBS. These samples contained some spherical pores, but many were rougher and misshapen. The strength values coincide with the smoothness and roundness of the voids at fracture initiation sites. These results suggest that small amounts of DBS may improve filler dispersion and result in a more benign flaw population, as well as a more rigid material. Material improvements from larger amounts of DBS may be obtained if processing techniques could be refined to eliminate the deleterious effects of the voids.

Indentation analyses of the fractured EBPADMA/Zr-ACP BFS specimens (3a−3d) reveal that the Knoop hardness of the composites increased with DBS content, as shown in Figure 4. The hardness values for samples with 8 and 10% by mass fraction DBS are not statistically significant, but all other values are significant by ANOVA analysis. The indentations were easily measured, and the large standard deviations would thus be expected to be due to local material differences. The increase in hardness upon addition of DBS

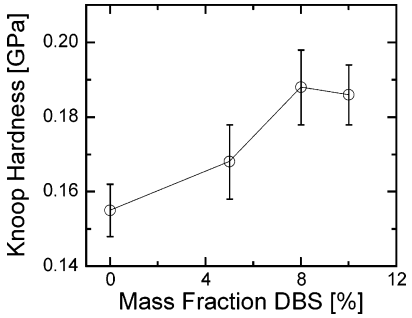

Figure 4. Knoop hardness as a function of DBS content in EBPADMA/Zr-ACP composites. The difference in the values for 8 and 10% by mass fraction DBS content are not statistically significant.

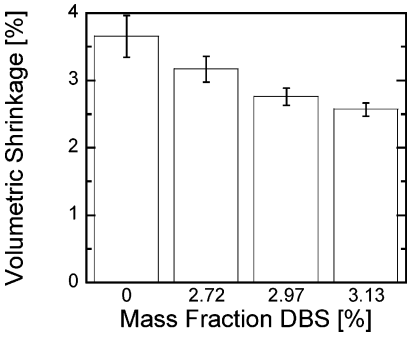

Figure 5. Volumetric shrinkage of EBPADMA/Zr-ACP composites containing various levels of DBS (as indicated).

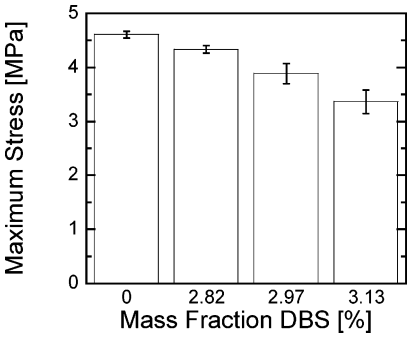

Figure 6. Maximum polymerization stress of EBPADMA/Zr-ACP composites containing various levels of DBS (as indicated).

may be partially due to the reduction in material flaws observed during the fractographic analyses, as well as the presence of the rigid three-dimensional DBS network.

Mercury dilatometry results for EBPADMA/Zr-ACP composites (samples 2a, 2b, 3b, and 5) are given in Figure 5 as a function of DBS concentration calculated with respect to the composition of the entire sample. These results reveal a statistically significant decrease in shrinkage upon addition of DBS. Volumetric shrinkage ranged from $3.7 \pm 0.3\%$ for the Zr-ACP composites containing no DBS to $2.6 \pm 0.1\%$ for the composites containing 3.13% by mass fraction DBS, suggesting that the DBS network may act to reduce shrinkage during polymerization. This, in turn, should cause a reduction in polymerization stress.

Results from the stress measurements, shown in Figure 6, complement the shrinkage results and show that the maximum stress decreases with increasing DBS concentration. Because the tensometer was unable to accommodate highly viscous samples, a loading of 43% Zr-ACP (2.82% DBS) had to be used for the tensometer measurements in lieu of

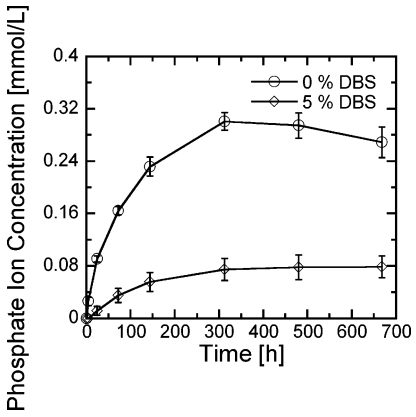

Figure 7. Phosphate ion concentration profile.

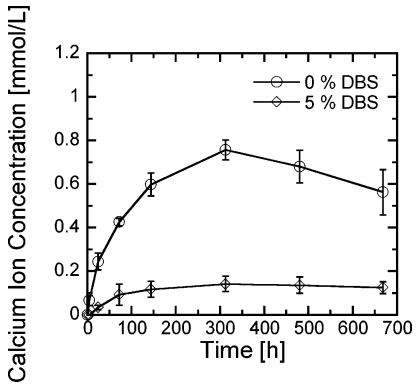

Figure 8. Calcium ion concentration profile.

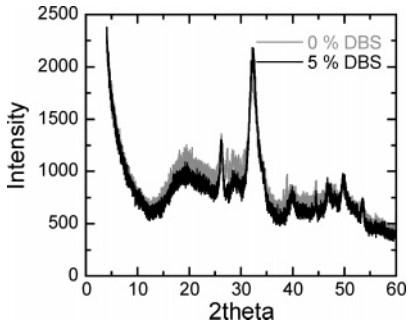

Figure 9. XRD pattern of composite specimens soaked for 668 h in a HEPES-buffered saline solution.

Table 4. Biaxial Flexural Strength of Cured EBPADMA/Zr-ACP Composite Specimens Both Dry and after Soaking for 668 h in a HEPES-Buffered Saline Solution (Standard Deviations Shown in Parentheses)

sample	BFS [MPa]
3a (dry)	59.5 (5.7)$^{A\,a}$
3a (soaked)	35.4 (3.4)^{B}
3b (dry)	83.0 (3.7)^{C}
3b (soaked)	33.4 (1.5)^{B}

^{a} Different superscript capital letters indicate statistical differences ($P < 0.05$).

the 45% Zr-ACP sample used in the dilatometry studies; however, the other compositions were identical. The maximum stress ranged from 4.6 ± 0.1 MPa for the samples without DBS to 3.4 ± 0.2 MPa for the samples containing 3.13% by mass fraction DBS. Surprisingly, the shrinkage stress and volumetric shrinkage do not appear to be affected by the total filler loading, which is highest in the samples with 2.72% DBS (47.7% filler) and 2.82% DBS (45.8% filler), which rules out the possibility that the reductions in both shrinkage and stress are actually due to higher filler loadings.

Recalling the vinyl conversion studies, it was shown that there were no significant differences in vinyl conversion among the EBPADMA/DBS/Zr-ACP composites containing the same amount of Zr-ACP. Increasing the amount of Zr-ACP, however, was found to decrease the conversion, presumably due to higher viscosities, more entrapped air, and/or reduced clarity. While a reduction in vinyl conversion might be expected to be accompanied by a reduction in shrinkage, the dilatometer and tensometer studies indicate that the samples with the highest filler loading were not necessarily the samples with the lowest shrinkage. This indicates that the reductions in shrinkage and shrinkage stress observed upon addition of DBS are not simply due to lower vinyl group conversion. It should be noted that slight differences in conversion between the dilatometer/tensometer specimens and the vinyl conversion specimens might be expected due to differences in conditions between the Caulk/Denstply and the Triad 2000 curing units. Although both units operate at maximum wavelengths of approximately 470 nm, there is some slight heating of the specimen in the Triad 2000 unit, as well as differences in distances between light source and specimen, which may lead to small discrepancies in degree of vinyl group conversion. These differences, however, would not be expected to alter the trends, but rather to shift the values.

The ion concentration release profiles for EBPADMA composites containing 40% by mass fraction Zr-ACP and 0 or 5% DBS (samples 3a and 3b) are shown in Figures 7 and 8. The DBS-containing samples exhibited significantly reduced release of both calcium and phosphate ions and slower initial release. X-ray diffraction patterns of the composites after 668 h of soaking are shown in Figure 9 and indicate that both types of composites converted into poorly crystalline apatite as evidenced by the presence of several spikes in the diffraction pattern. The differences in the ion release profiles, however, suggest that the kinetics of conversion were highly different. One plausible explanation is that the hydroxyl groups of the DBS inhibit ion release by binding with the calcium and phosphate ions. It is also possible that the samples containing DBS absorbed more solution, thereby accelerating the conversion of the ACP into apatitic material. Comparison of specimen mass before and after soaking revealed that the DBS-containing specimens had an average of a 6.6 ± 0.3% mass gain compared to 4.5 ± 0.8% for the samples without DBS, indicating that the samples containing DBS did absorb more solution. Future efforts may involve a systematic XRD/FTIR analysis of the specimens during the soaking period to determine the kinetics of the conversion into apatitic forms.

Both EBPADMA/Zr-ACP composites with and without DBS exhibited a significant decrease in biaxial flexural strength after soaking for 668 h in a HEPES-buffered saline solution as shown in Table 4. The samples containing DBS, however, suffered a larger decrease in biaxial flexural strength than the specimens without DBS, although the final strength values were indistinguishable. The larger reduction

in the samples containing DBS is likely due to the higher solution absorption, as the liquid swells the composite introducing defects and reducing the cross-link density of the polymer network. The reasons for the higher water uptake in the DBS-containing composites are not yet fully understood, but the DBS network itself may also reduce the cross-link density of the polymer network resulting in a more open network capable of absorbing higher amounts of solution.

Conclusions

The work presented here reveals that while DBS has little effect on the vinyl conversion of EBPADMA/Zr-ACP composites, it may act to increase the biaxial flexural strength and hardness of the dry composites, improve filler dispersion, and reduce polymerization shrinkage and stress. Ion release studies, however, indicate that DBS significantly decreases the ion release capabilities of EBPADMA/Zr-ACP composites, suggesting that DBS may be more appropriate for glass- or silica-filled composites, or perhaps for use in a different bioactive filler/resin system. At this point it remains unclear whether the improvements in biaxial flexural strength and shrinkage and stress development properties are due to the DBS network or some other unknown effect of the DBS. However, these results suggest that organogelators may be useful additives for increasing the strength and reducing the polymerization shrinkage of filled dental composites.

Disclaimer. Certain commercial materials and equipment are identified in this work for adequate definition of the experimental procedures. In no instance does such identification imply recommendation or endorsement by the National Institute of Standards and Technology or the American Dental Association Foundation or that the material and the equipment identified is necessarily the best available for the purpose.

Acknowledgment. This work was supported by an interagency agreement of the National Institute of Standards and Technology with the National Institute of Dental and Craniofacial Research (NIDCR, Y1-DE-1021-04). Additional funding was received through NIDCR grants DE-14534 and DE-13169-05, and from the National Research Council Postdoctoral Associate Program. These efforts are part of the dental research program conducted by the National Institute of Standards and Technology in cooperation with the American Dental Association Foundation. We are grateful for the gifts of EBPADMA from Esstech (Essington, PA) and DBS from Milliken Chemicals (Spartanburg, SC).

CM048340X